Gastrointestinal Uptake of Biodegradable Microparticles: Effect of Particle Size

Manisha P. Desai,[1,2] Vinod Labhasetwar,[1,2] Gordon L. Amidon,[2] and Robert J. Levy[1,2,3]

Received July 8, 1996; accepted September 9, 1996

Purpose. To investigate the effect of microparticle size on gastrointestinal tissue uptake.

Methods. Biodegradable microparticles of various sizes using polylactic polyglycolic acid (50:50) co-polymer (100 nm, 500 nm, 1 μm, and 10 μm) and bovine serum albumin as a model protein were formulated by water-in-oil-in-water emulsion solvent evaporation technique. The uptake of microparticles was studied in rat *in situ* intestinal loop model and quantitatively analyzed for efficiency of uptake.

Results. In general, the efficiency of uptake of 100 nm size particles by the intestinal tissue was 15–250 fold higher compared to larger size microparticles. The efficiency of uptake was dependent on the type of tissue, such as Peyer's patch and non patch as well as on the location of the tissue collected i.e. duodenum or ileum. Depending on the size of microparticles, the Peyer's patch tissue had 2–200 fold higher uptake of particles than the non-patch tissue collected from the same region of the intestine. Histological evaluation of the tissue sections demonstrated that 100 nm particles were diffused throughout the submucosal layers while the larger size nano/microparticles were predominantly localized in the epithelial lining of the tissue.

Conclusions. There is a microparticle size dependent exclusion phenomena in the gastrointestinal mucosal tissue with 100 nm size particles showing significantly greater tissue uptake. This has important implications in designing of nanoparticle-based oral drug delivery systems, such as an oral vaccine system.

KEY WORDS: oral; drug delivery; nanoparticles; Peyer's patches; size exclusion; vaccine.

INTRODUCTION

Biodegradable particulate carrier systems are of interest as a potential means for oral delivery to enhance drug absorption (1–4), improve bioavailability (5), targeting of therapeutic agents to particular organ and reduce toxicity (6,7), to improve gastric tolerance of the agents irritant to the stomach (8) and as a carrier for antigen in oral immunization (9). The Gut Associated Lymphoid Tissue (GALT), such as lamina propria, intraepithelial lymphocytes, isolated lymphoid follicles, and Peyer's patches are the primary immune system of the gastrointestinal tract (10,11). Orally administered particulate matters gain entry into the follicle associated epithelium overlying the dome region of Peyer's patches, via M cells (12–15). Several studies have demonstrated the uptake of orally administered polystyrene particles by the Peyer's patch tissue and their subsequent translocation to discrete anatomical compartments, such as the mesenteric lymph vessels, lymph nodes, and in lesser amounts in the liver and the spleen (16–18) which could trigger both mucosal and systemic immune responses. Microparticles, in addition to protecting antigen from gastric pH and proteolytic enzymes also act as an adjuvant because they produce an elevated immune response compared to soluble antigen (9,19–21).

Several studies have been carried out with various types of polymeric materials to investigate the factors influencing the gastrointestinal uptake of microparticles (18,22–24). Size of the microparticles in studies by Jani et al. using polystyrene particles has shown to have influence on efficiency of uptake (18). Following oral gavage, the extent of absorption of particles smaller than 100 nm was significantly higher than larger size particles with more than 60% of the total uptake from the Peyer's patches of the small intestine (18,25). Thus by using optimal size microparticles as a carrier system for antigen, the immune response could be improved. Therefore, our objective in this study is to investigate the efficacy of uptake of various size biodegradable PLGA microparticles, containing BSA as a model antigen, by the gastrointestinal tissue. The goals in this study are to: (i) formulate and characterize microparticles of 100 nm, 500 nm, 1 μm and 10 μm diameter, (ii) evaluate uptake of various size microparticles in *in situ* rat intestinal loop model, and (iii) study histological localization of various size microparticles following *in situ* experiment.

MATERIALS

Polylactic polyglycolic acid copolymer (PLGA, 50 : 50, MW-100,000, inherent viscosity: 1.07 measured in hexafluoroisopropanol) was obtained from Birmingham polymers Inc., AL. Other chemicals used were polyvinyl alcohol (PVA, MW: 30,000–70,000) and bovine serum albumin (BSA, Fraction V) obtained from Sigma Chemical Co. (St. Louis, MO); 6-coumarin from Polyscience Inc., (Warrington, PA) and sodium salt of 1-heptane sulfonic acid from Aldrich Chemical Co., (Milwaukee, WI). Methylene chloride, chloroform, acetonitrile, ethyl acetate were of either HPLC grade or of an American Chemical Society Reagent grade.

Animals

Male Sprague Dawley adult rats (200–250 g wt., 12–15 weeks old) were obtained from the reproductive services at the University of Michigan. Experiments were carried out in compliance with the regulations of University Committee on Use and Care of Animals (UCUCA) at the University of Michigan.

METHODOLOGY

Formulation of PLGA Nanoparticles and Microparticles

Microparticles of various sizes of an average diameter of 100 nm, 500 nm, 1 μm and 10 μm were formulated by optimizing formulation parameters as shown in Table I. In brief, an aqueous BSA solution (10% w/v) was emulsified in a polymer solution (3–15% w/v PLGA) in methylene chloride, using a microtip probe sonicator set at 65 watts of energy output (Miso-

[1] University of Michigan, Division of Pediatric Cardiology, Ann Arbor, Michigan 48109.
[2] University of Michigan, College of Pharmacy, Ann Arbor, Michigan 48109.
[3] To whom correspondence should be addressed.

0724-8741/96/1200-1838$09.50/0

Table I. Formulation and BSA Loading of Different Size Microparticles

PLGA Solution (w/v %)	PVA Solution (w/v %)	Emulsion (w/o/w)	Desired Diameter	Actual Diameter mean ± s.e.m. n = 50	BSA Loading, (wt %) mean ± s. e. m. n = 3	Encapsulation Efficiency, (%) mean ± s. e. m. n = 3
3.0	2.5	Sonicator	100 nm	116.0 ± 5.0 nm	7.82 ± 0.23	31.28 ± 0.9
15.0	0.5	Microfluidizer	500 nm	528.0 ± 20.0 nm	4.92 ± 0.03	19.69 ± 0.1
6.0	0.5	Homogenizer	1 μm	1.1 ± 0.1 μm	4.47 ± 0.53	17.89 ± 2.1
3.0	2.5	Vortex	10 μm	9.4 ± 0.2 μm	5.48 ± 0.04	21.80 ± 0.2

nix Inc. Model XL 2020™, Farmingdale, NY) for 10 min. over an ice bath to form a water-in-oil (w/o) emulsion. The polymer solution also contained 0.05% w/v 6-coumarin as a fluorescent marker. The o/w emulsion was further emulsified into an aqueous PVA solution (0.5–2.5% w/v) to form a water-in-oil-in-water (w/o/w) emulsion.

The w/o/w emulsion was stirred over a magnetic stir plate overnight at room temperature to evaporate methylene chloride. Particles of 100 nm were recovered by ultracentrifugation (Beckman model XL-70, Arlington Hts., IL) at 100,000 g for 20 minutes. Larger size microparticles were recovered by centrifugation at 3000 rpm for 20 minutes (Ice Centra-7R, International Equipment Co., Needham Hts, MA). The particles were washed three times with water to remove PVA and unencapsulated BSA, and resuspended in water prior to lyophilization.

Characterization of Microparticles

Particle Size Distribution

Particles of 100 nm diameter were characterized for size distribution using a dynamic laser defractometer (NICOMP, Model 370, Hiac/Royco Instruments Division, Santa Barbara, CA). Optical microscopy (Olympus CHT-001, Olympus Corporation, Lake Success, NY) was used to measure the size distribution and diameter of other size particles. In addition, scanning electron microscopy (SEM) was performed to determine the surface topography of the particles. A sample of microparticles was placed on a double stick tape over aluminum stubs to get an uniform layer of particles. Sample was gold coated using a sputter gold coater (Denton Vacuum Inc., Cherry Hill, NJ) at 40 milliampere current and 50 millitorr pressure for 200 seconds at the thickness of 300 A°. Gold coated particle samples were cooled over dry ice prior to SEM observations to avoid their melting under high magnification due to the electron beam exposure (Hitachi S570, Cherry Hill, NJ).

BSA Loading of Microparticles

In a typical procedure, a sample of microparticles (5–10 mg) dissolved in 5 ml chloroform was extracted five times with each extract of 5 ml water. The combined aqueous extracts was assayed for BSA content using the coomassie blue micro BioRad® (BIO-RAD Laboratories, Hercules, CA) protein assay.

SDS-Polyacrylamide Gel Electrophoresis (SDS-PAGE)

BSA extracted from microparticles as described above was lyophilized and analyzed by SDS- PAGE to see changes, if any, in BSA following it's encapsulation into microparticles. Samples were mixed with 1.5 M Tris-HCl buffer (pH 6.8) containing 10% SDS, 40% glycerol, 0.02% bromophenol blue and 5% 2-mercaptoethanol, were heated at 95°C for 5 min. and subjected to electrophoresis at 40 mA in a vertical slab Mini-PROTEAN® II gel (BIO-RAD Laboratories, Hercules, CA). Proteins were visualized by silver staining in water, methanol and acetic acid (30 : 50 : 10 by volume).

In Vitro Release of BSA from Microparticles

The *in vitro* release of BSA from PLGA microparticles was carried out under physiologic condition at 37°C. A sample of microparticles (5 mg) suspended in 5 ml phosphate buffer (pH 7.4) was placed in the donor chamber of the double diffusion cells, separated by a 0.1 μm Millipore® (Type VV, Bedford, MA) membrane. The buffer in the receiver chamber was replaced periodically with fresh buffer. The samples were assayed for the BSA levels using micro BioRad® protein assay.

In Vitro Release of 6-Coumarin from Nanoparticles

A suspension of 100 nm particles (4 mg/ml) in PBS was placed on a rotary shaker at 37°C for two hours. Periodic samples were subjected to centrifugation at 10,000 g and the supernatant was analyzed for the released 6-coumarin by HPLC assay as described later.

Acute Animal Model Studies

Uptake of Microparticles in Rat In Situ *Intestinal Tissue Loop Model*

Animals were fasted with free access to water for 18–24 hours prior to the experiments. Rats were given general anesthesia with an intraperitoneal injection of sodium pentobarbital (6.5 mg/100 g body weight). A midline abdominal incision exposed the small intestine. Two separate intestinal segments (duodenal and ileal) of 15–20 cm length were created by incising approximate length of small bowel, that were then clamp sealed with a Kelly clamp. These segments of intestine were infused with about 100 ml of normal saline to wash off the intestinal food contents and were ligated with 2.0 Ethicon sutures (Ethicon Inc., Somerville, NJ) to form two loops, one in the region of duodenum and other in the region of ileum (26).

An aliquot of the microparticle suspension (4 mg/ml) in normal saline was infused into these segments using a syringe. After two hours, the loops were opened, microparticle suspension was drained out from each loop and the segments were

flushed with 100 ml normal saline. Loops were isolated and cut open through the mid-line incision. Mucin was scraped off with a metal spatula from the inner lining of intestine to remove the adsorbed particles. The Peyer's patch and the non-patch tissue were isolated from the intestine using a 4 mm diameter Baker's biopsy punch (Cummins Dermatologicals Inc., Miami, FL). The tissue samples were immersed in normal saline for an hour to wash off the residual mucin layer (24). Each tissue sample was blotted gently, weighed, and frozen until taken for further analysis. The length of the intestinal segment into which the microparticle suspension was infused was measured to determine the total amount of microparticles infused into each segment.

In a separate study, a control experiment was carried out by infusing a 6-coumarin solution (0.51 μg/ml) into the rat intestinal loops under identical conditions as those used for the microparticle infusion experiment described above. This is the amount of 6-coumarin that is released from the 100 nm particles in two hours under *in vitro* physiologic conditions at a 4 mg/ml nanoparticle concentration. The control experiment was carried out to ensure that the 6-coumarin estimated in the tissue was associated with the microparticles taken up by the tissue and not due to the uptake of 6-coumarin that is released from the microparticles during two hours of experimental period. The amount of 6-coumarin in each of the tissue samples was quantitated by HPLC as described below.

Animal Model Retrieval Analysis

Extraction of 6-Coumarin from Tissue Samples

Each tissue sample was homogenized separately with 1 ml of double distilled water using a high speed homogenizer (Stir-Pak®, Lab mixer, Cole-Parmer Instruments Co., Chicago, IL) for about 15 minutes over an ice-bath. The homogenate was extracted five times with 3 ml ethyl acetate at each extraction step. The combined extracts from each tissue sample were evaporated using a SpeedVac evaporator (SpeedVac® Plus SC110A, Savant Instruments, Inc., Farmingdale, NY). The residue was reconstituted with 200 μl acetonitrile for HPLC analysis.

HPLC Assay for 6-Coumarin

The Waters (Milford, MA) HPLC system consisted of a pump (model 501), an autosampler (Wisp model 712), a data module (model 740), and a μBondapak C_{18} column with 10 μm packing. Separations were achieved using acetonitrile : water : 1-heptane sulfonic acid sodium salt (50 : 50 : 0.005 M) as a mobile phase. The eluents were monitored using a scanning fluorescence detector (model 470,) at 450 nm excitation wavelength and 490 nm emission wavelength.

For each batch of microparticles, a standard curve for 6-coumarin was constructed by spiking different weight concentrations of microparticles (10 μg to 80 μg) followed by extraction of 6-coumarin and analysis by HPLC as discussed above. The amount of microparticles (μg) taken up by each tissue sample was calculated from the standard curve for corresponding size of microparticles.

The number of particles taken up by the Peyer's patch and the non patch tissue was estimated from the weight of microparticles taken up by the tissue using the following equation (27):

$$\text{Number of particles} = \frac{w \times k \times 10^9}{d^3} \quad (1)$$

where, w is the mass of particle uptake in μg per sq. mm area of the tissue, d is the diameter of particles in μm, and k is the factor (1.426) that takes into account the density (gm/cc) of the polymer used.

The Efficiency of Particle Uptake in the Rat In Situ Model

The total surface area of the intestinal loop in the *in situ* experiment that was used to infuse the microparticles was calculated from the length and diameter. From the total area of the intestinal loop as calculated above and the total amount of microparticles infused, a theoretical dose of microparticles per unit area of the intestine exposed was calculated (μm/mm^2). The estimated dose calculated as above was 6.5 μg microparticles per sq. mm area of intestinal tissue exposed. The efficiency of uptake of microparticles for each particle size was determined from the actual uptake of microparticles ('w' in μg/mm^2) and the estimated dose of the microparticles as calculated above.

Histology

Tissue samples were embedded in a cryostat medium (OTC, TEK II 4583, Miles Inc., Elkhart, IN) and snap frozen in isopentane and then in liquid nitrogen. Tissue sections of 7 μm thickness were cut using a microtome cryostat (Model CTI, International Equipment Company, Needham Hts., MA) at −18 to −20°C. The sections were fixed on glass slides by warming for 30 seconds. The sections were mounted in a drop of Vectashield® (Vector Labs, Inc., Burlingame, CA) and were viewed under a fluorescence microscope (Model Orthoplan, Leitz, W. Germany) using a FITC filter (wavelength 450–490 nm).

Statistical Methods

Results are presented as mean ± s.e.m. Statistical comparisons were made with students t-test at a 99% confidence level. Difference between the tissue uptake of microparticles was considered statistically significant at $p < 0.01$.

RESULTS

Formulation and Characterization of Various Size Microparticles

Microparticles of the desired particle size were obtained by optimizing various formulation parameters and energy source input used to form the w/o/w emulsions. As can be seen from the SEM analysis, all four sizes of particles formulated were spherical with smooth uniform surfaces (Fig. 1) with more than 80% particles in the desired size range. In general, BSA loading was in the range of 4% to 8% w/w with encapsulation efficiency in the range of 15% to 32%. This variation in BSA loading is due to differences in the composition and the emulsification protocol used.

In this study, all size nano/microparticles demonstrated *in vitro* an initial burst release of 10% to 20% of the encapsulated

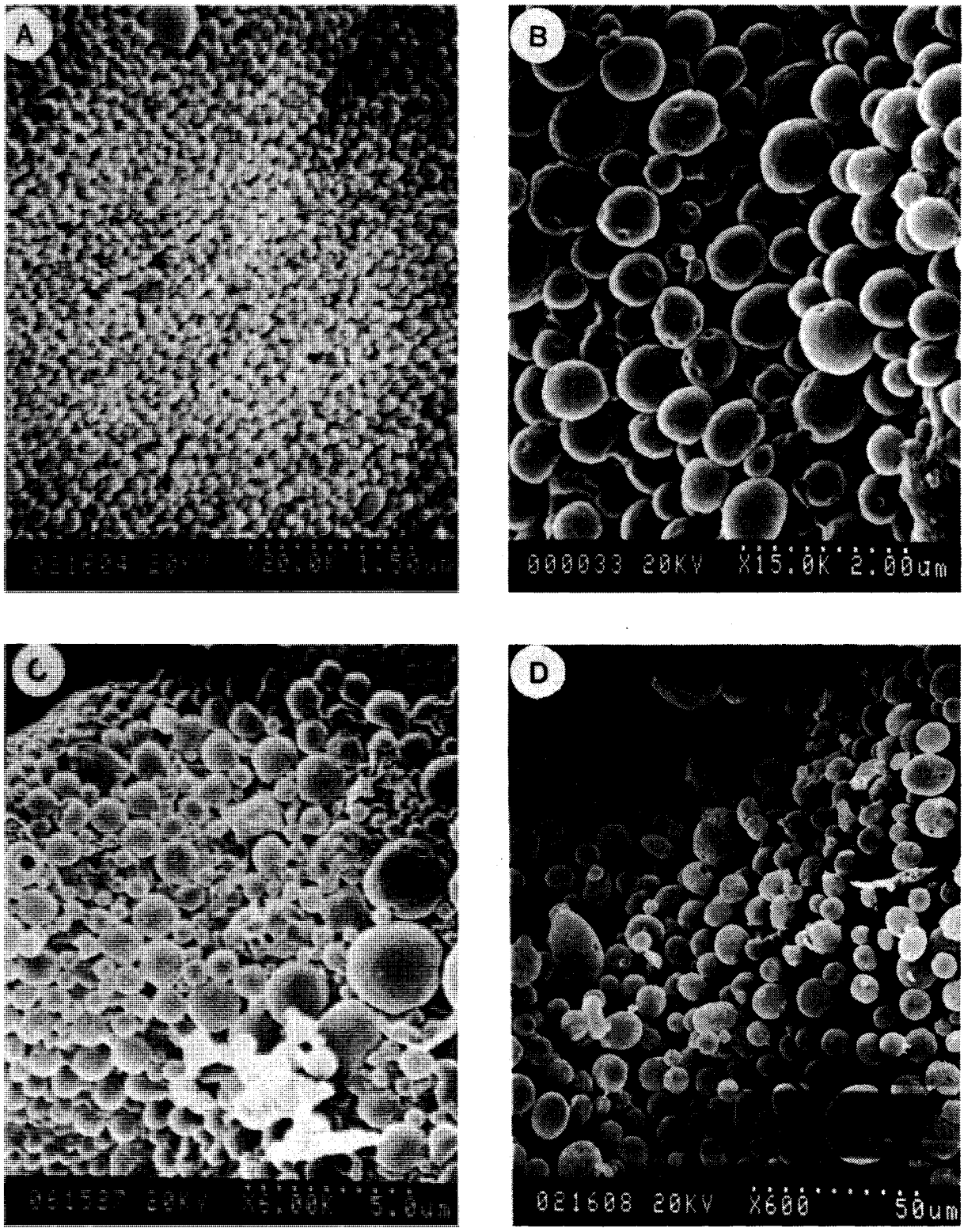

Fig. 1. SEM analysis of microparticles a) 100 nm, b) 500 nm, c) 1 μm, and d) 10μm.

BSA within first two days. The subsequent release of BSA up to 20 days was at a slower releasing rate during which only an additional 10% to 20% of the BSA was released. This slow release phase was followed by a second burst release from day 20–60 possibly due to hydrolytic erosion of the polymer matrix (Fig. 2). The difference in the burst effect for various size microparticles seems to be due to variation in the formulation composition and conditions. SDS-PAGE analysis of the encap-

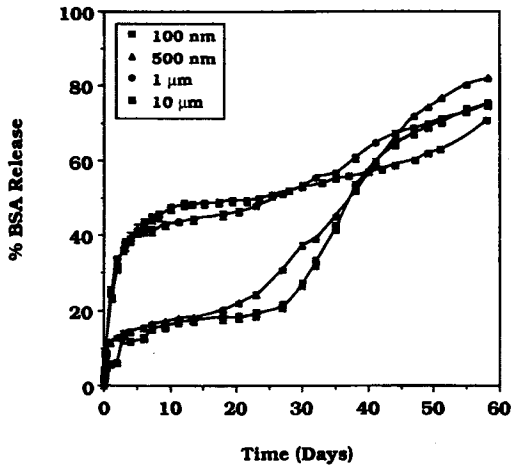

Fig. 2. *In Vitro* release of bovine serum albumin from various size PLGA microparticles (n = 3).

sulated protein shows bands that correlated with intact BSA indicating that the protein does not interact chemically with the matrix material into PLGA microparticles or does not lead to a significant irreversible aggregation of the protein.

In Situ Uptake of Microparticles

The microparticle uptake by the Peyer's patch tissue was significantly higher ($p < 0.001$) for 100 nm particles compared to all other sizes of particles (Fig. 3). In addition, the Peyer's patch tissue appears to have comparatively higher uptake of particles than nonpatch tissue. Furthermore, the Peyer's patch and the nonpatch tissue from the ileum had comparatively higher uptake of microparticles than the identical tissues collected from the region of duodenum ($p < 0.001$).

For each particle size range, the uptake of microparticles was calculated in terms of their number from the diameter, the weight of the microparticles taken up by the tissue, and the density of the PLGA polymer as per equation (i). Nanoparticles of 100 nm diameter were found to be present at levels which were several folds higher in number compared to larger size particles. For example, the number of the 100 nm particles per sq. mm of Peyer's patch is 4×10^6 fold higher than 10 μm size microparticles and 6.7×10^3 fold higher than 1 μm particles (Table II). The tissue 6-coumarin levels in the group infused with nanoparticle were several fold higher than the tissue coumarin levels detected in the control experiment, indicating that 6-coumarin levels detected in the tissue were mainly due to the coumarin contained within the particles (Fig. 4).

Histological Evaluation of Microparticle Uptake

Histological examination of the Peyer's patch and the non patch samples showed a higher level of uptake for the 100 nm particles compared to larger size particles. Particles of 100 nm diameter were seen diffused throughout the submucosal layer as well as on the serosal side of the Peyer's patch. Microparticles of 500 nm, 1 μm and 10 μm sizes were taken up to a much lesser extent and were mainly seen localized in the epithelial lining of the Peyer's patch and the nonpatch microvilli (Fig. 5A–J).

DISCUSSION

The efficiency of uptake of microparticle encapsulated antigen by the gastrointestinal lymphoidal tissue is a key factor in the successful development of an oral vaccine system. Our studies demonstrated that the 100 nm size particles have a significantly higher efficiency of uptake by the intestinal tissue in terms of their total mass and the number compared to larger size particles. Thus, it implies that the total mass of the antigen uptake by the tissue encapsulated in the smaller size nanoparticles will be significantly higher. Histological examination of the Peyer's patch and the non-patch tissue shows that nanoparticles were distributed into the submucosal layers as compared to larger size particles which were mostly aligned at the epithelial linings. Thus it seems that there is a particle size dependent exclusion phenomena with smaller size particles more likely to be internalized inside the cells and tissue. This has significant importance in the development of a successful oral vaccine system because oral immunization results in poor immune

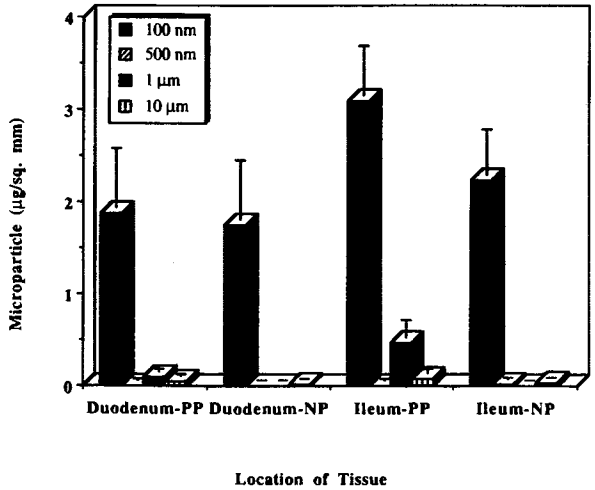

Fig. 3. *In situ* uptake of microparticles by rat intestinal tissue in weight (μg) of particles per sq. mm area of rat intestinal tissue. PP = Peyer's patch and NP = non-patch tissue (n = 15–20).

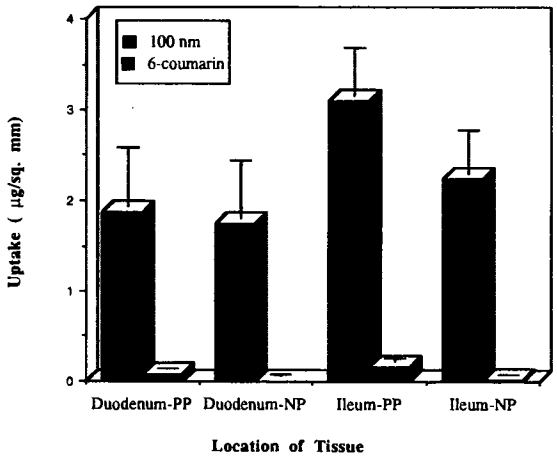

Fig. 4. Comparative *in situ* uptake of 100 nm particles and 6-coumarin from Peyer's patch and non-patch tissue; $p < 0.001$ (n = 10).

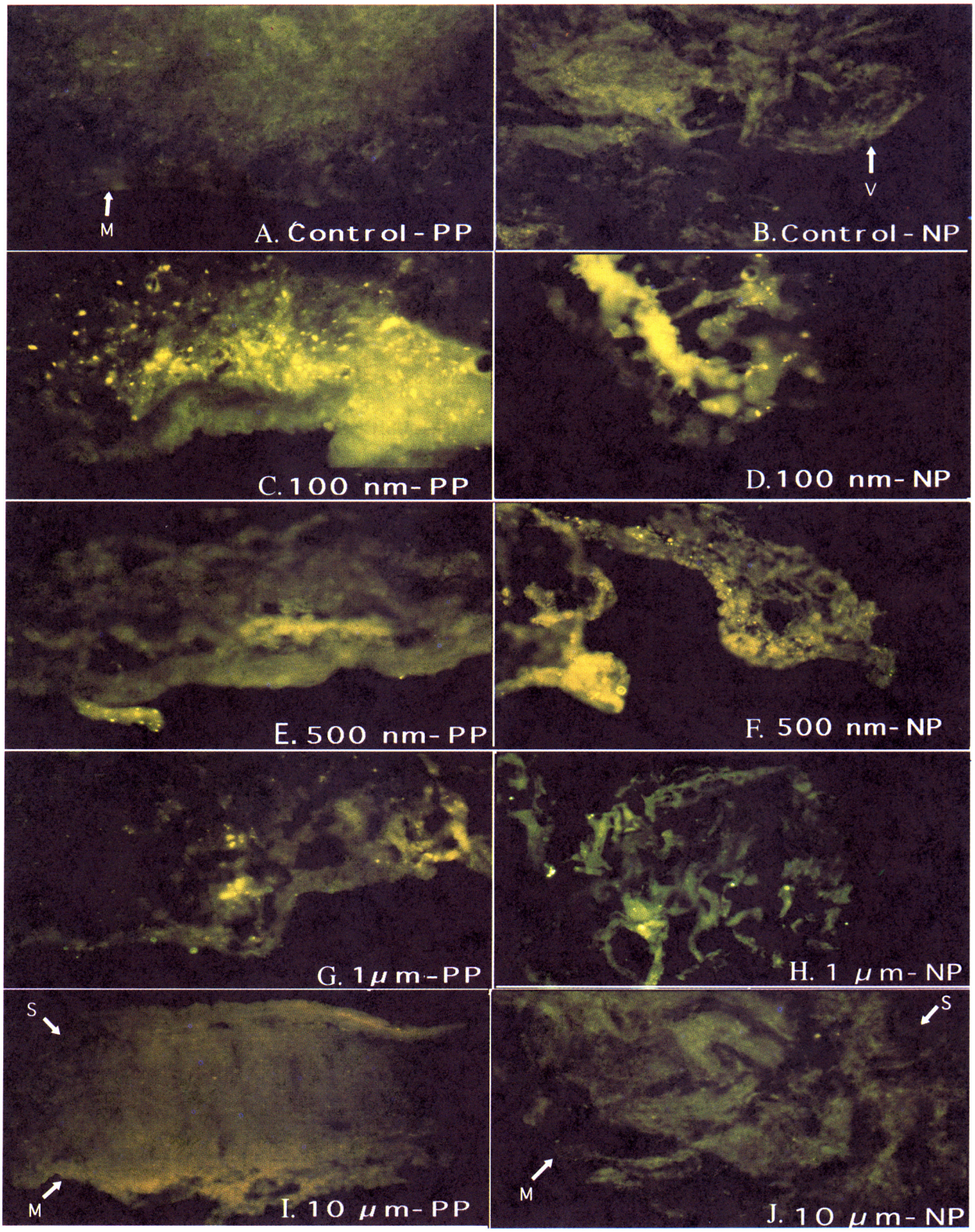

Fig. 5. Histological analysis of Peyer's patch and non-patch tissue exposed to various size microparticles in rat *in situ* experiment. PP = Peyer's patch and NP = non patch tissue, M = mucosa, S = serosa and V = villi.

response mainly due to very low efficiency of uptake of an orally administrated antigen.

In other studies, investigators have used particles in micron size range and demonstrated that PLGA (85:15) particles >5 μm in diameter cannot traverse in the Peyer's patch and are not seen systemically (28). Similar studies (not using nanoparticles) by Ebel (24) showed greater uptake of <5 μm fluorescent polystyrene latex particles in the Peyer's patch in mice. It is

Table II. Microparticle Uptake in Number/mm^2 and % Efficiency of Uptake from Rat Intestinal Tissue[a]

Particle Size[b]	Microparticle (Number/mm^2);[% Efficiency, mean ± s.e.m.]			
	Duodenum-PP	Ileum-PP	Duodenum-NP	Ileum-NP
100 nm	2.7×10^9 [30.07 ± 10.30]	4.4×10^9 [49.57 ± 8.34]	2.5×10^9 [27.88 ± 10.30]	3.2×10^9 [35.69 ± 7.85]
500 nm	8.4×10^4 [0.12 ± 0.06]	7.9×10^4 [0.11 ± 0.06]	4.4×10^4 [0.06 ± 0.02]	1.9×10^5 [0.27 ± 0.12]
1 μm	1.3×10^5 [1.51 ± 0.51]	6.5×10^5 [7.45 ± 3.05]	5.9×10^2 [0.01 ± 0.01]	1.3×10^3 [0.01 ± 0.01]
10 μm	0.7×10^2 [0.80 ± 0.19]	1.2×10^2 [1.33 ± 0.70]	0.2×10^2 [0.26 ± 0.07]	0.4×10^2 [0.48 ± 0.11]

Note: Dose = 6.25 μ/mm^2; n = 15 − 23 samples. PP = Peyer's Patch; NP = Non Patch Tissue.
[a] $p < 0.001$; 116 nm particles vs. 519 nm, 1 μm and 9.4 μm particles.
[b] Nominal Sizes; Actual mean diameters were 116 nm, 519 nm, 1 μm and 9.4 μm.

also hypothesized by Florence et al. (14) that nanoparticles because of their smaller size would also have an efficient disposition via Peyer's patches to other lymphatic organs such as to the mesenteric lymph nodes and to spleen to induce systemic immune response.

Smaller size nanoparticles could also have efficient gastrointestinal tissue uptake by other routes, such as uptake by intracellular pathways. Nanoparticles could gain entry in the tissue through intracellular spaces and especially in larger defects of the mucosa. Several other investigators too noticed this phenomena with smaller size particles (29,30). In a morphological study, Sanders and Ashworth (16) found that 200 nm latex particles were taken up into jejunal absorptive cells of adult rats. The particles were observed in intact intracellular vesicles and were then discharged into the lamina propria.

Although there is no proposed receptor based mechanism for the uptake of particulate matter by the M cells, particles may be taken up by a non specific endocytosis. Several physical properties of microparticles could influence their interactions within the M cells and also other cells of the gastrointestinal tissue. Other investigators have also demonstrated that hydrophobic microparticles have higher efficiency of uptake compared to hydrophilic particles (28). Thus it seems that apart from particle size and hydrophobicity, factors such as surface charge and other interfacial and surface properties of microparticles could also influence their uptake by the gastrointestinal tissue. Jani and co-workers have demonstrated that uptake of non-ionized polystyrene nanoparticles was greater than the uptake of negatively charged (carboxylated) particles by the rat gastrointestinal tissue after oral gavage (17).

Thus, nanoparticles could prove to have potential applications in oral drug delivery including vaccine in oral immunization due to their efficient uptake by the GALT, and also to improve oral bioavailability of therapeutic agents (5). In addition, oral administration of nanoparticles encapsulated agent could provide sustained drug effect because these can become trapped in the microvilli, thus prolonging their gastrointestinal transit time. The slow breakdown of the polymer would provide sustained release of therapeutic agent over a period of time. An enteric coated capsule or time release capsule could be used to deliver these nanoparticles, bypassing gastric pH. Although the efficiency of uptake of 100 nm particles observed in this study is under optimally controlled experimental conditions, *in vivo* it could be influenced by several other factors such as the presence of food, interaction of nanoparticles with luminal contents and contact of nanoparticles with gastrointestinal tissue, however the size exclusion dependent phenomenon will remain consistent with the findings of this study.

CONCLUSIONS

i. This study demonstrated that 100 nm size nanoparticles show significantly greater uptake than larger size nano/microparticles.

ii. The increased uptake of smaller particles could broaden the uses for nanoparticle delivery systems to include intestinal administration of vaccines, proteins and peptides (such as insulin) and DNA for transgene delivery.

iii. The increased uptake of smaller particles by GALT implies that smaller nanoparticles may be particularly well suited for use with vaccines.

ACKNOWLEDGMENTS

This work was partially supported by TSRL Inc., Ann Arbor, MI, under a subcontract from the U.S. Army SBIR program (V. L.) (Contract # DAMD17-95-C-5060), and by the Matrigen Corporation (R. J. L.), Ann Arbor, MI. Authors thank Ardith Bates for her secretarial assistance.

REFERENCES

1. P. Couvreur, B. Kante, M. Roland and P. Speiser. *J. Pharm. Sci.* **68 (12)**:1521–1524 (1979).
2. P. Couvreur, V. Lenaerts, D. Leyh, P. Guiot and M. Roland. In Microspheres and Drug Therapy. Pharmacuticals, Immunological and Medical Aspects. Edited by S. S. Davis, L. Illum, J. G. McVie and E. Tomlinson., Elsevier Science Publishers B. V. 103–115 (1984).
3. J. Kreuter. *Inter. J. Pharm.* **14**:43–58 (1983).
4. L. Illum, S. S. Davis, R. H. Muller, E. Mak and P. West. *Life Sci.* **40**:367–374 (1987).
5. P. Maincent, R. Le Verge, P. A. Sado, P. Couvreur and J. P. Devissaguet. *J. Pharm. Sci.* **75**:955–958 (1986).
6. P. A. Kramer and T. Burnstein. *Life Sci.* **19**:515–520 (1976).
7. J. J. Marty, R. C. Oppenheim and P. P. Speiser. *Pharm. Acta Helv.* **53**:17–23 (1978).
8. C. M. Adeyeye, J. D. Bricker, V. D. Vilivalam and W. I. Smith. *Pharm. Res.* **13**:784–793 (1996).
9. J. Mestecky, Z. Moldoveanu, M. Novak, W. Q. Huang, R. M. Gilley, J. K. Staas, D. Schafer and R. W. Compans. *J. Control. Rel.* **28**:131–141 (1994).
10. C. A. Gilligan and A. L. Wan Po. *Inter. J. Pharm.* **75**:1–24 (1991).
11. D. T. O'Hagan, K. J. Palin and S. S. Davis. *CRC Critical Reviews in Therapeutic Drug Carrier Systems.* **4**:197–220 (1987).
12. H. O. Alpar, W. N. Field, R. Hyde and D. A. Lewis, *J. Pharm. Pharmacol.* **41**:194–196 (1989).

13. M. E. LeFevre, J. W. Vanderhoff, J. A. Laissue and D. D. Joel. *Experientia.*. **34**:120–122 (1978).
14. A. T. Florence and P. U. Jani. In Pharmaceutical Particulate Carriers. Therapeutic Application. Edited by Alain Rolland, Marcel Dekker Inc. **61**:65–108 (1993).
15. J. Pappo and T. H. Ermak. *Clin. Exp. Immunol.* **76**:144–148 (1989).
16. E. Sanders and C. T. Ashworth. *Exp. Cell Res.* **22**:137–145 (1961).
17. P. Jani, G. W. Halbert, J. Langridge and A. T. Florence. *J. Pharm. Pharmacol.* **41**:809–812 (1989).
18. P. Jani, G. W. Halbert, J. Langridge and A. T. Florence. *J. Pharm. Pharmacol.* **42**:821–826 (1990).
19. D. S. Cox and M. A. Taubman. *Int. Archs Allergy Appl. Immun.* **75**:126–131 (1984).
20. O. Strannegard and A. Yurchision. *Int. Arch. Allergy.* **35**:579–590 (1969).
21. J. R. McGhee, J. Mestecky, M. T. Dertzbaugh, J. H. Eldridge, M. Hirasawa and H. Kiyono. *Vaccine* **10**:75–88 (1992).
22. M. E. LeFevre and D. D. Joel. In Intestinal Toxicology. Edited by C. M. Schiller. Raven Press. 45–56 (1984).
23. J. H. Eldridge, J. K. Staas, J. A. Meulbroek, J. R. McGhee, T. R. Tice and R. M. Gilley. *Mol. Immunol.* **28**:287–294 (1991).
24. J. P. Ebel. *Pharm. Res.* 7:848–451 (1990).
25. A. M. Hillery, P. U. Jani and A. T. Florence. *J. Drug Targetting.* **2**:151–156 (1994).
26. H. Tomizawa, Y. Aramaki, Y. Fujii, T. Hara, N. Suzuki, K. Yachi, H. Kikuchi and S. Tsuchiya. *Pharm. Res.* **10**:549–552 (1993).
27. R. H. Muller. In Colloidal carriers for controlled drug delivery and targeting. *CRC Press, Boston.* 43–45 (1991).
28. J. H. Eldridge, C. J. Hammond, J. A. Muelbroek, J. K. Staas, R. M. Gilley and T. R. Tice. *J. Control. Rel.* **11**:205–214 (1990).
29. C. Damge, C. Michel, M. Aprahamian, P. Couvreur and J. P. Devissaguet. *J. Control. Rel.* **13**:233–237 (1990).
30. M. Aprahamian, C. Michel, W. Humbert, J. P. Devissaguet and C. Damge. *Bio. Cell.* **61**:69–74 (1987).